

Chapter 19

Real-Time and Fast Retrieve the Coseismic Wave by GPS, Strong-Motion Combined Measurements and Broadcast Ephemeris

Rui Tu

Abstract In this study, we propose an approach of real-time and fast retrieving the coseismic waves by GPS, strong-motion combined measurements and broadcast ephemeris. Firstly, the velocity observation equations and state equations of the strong-motion measurements are introduced into Precise Point Positioning (PPP) solution model, the baseline shifts of the strong-motion are real-time estimated as unknown parameters like other positioning parameters by a Kalman filter. Then, the true velocity wave was retrieved by correcting the estimated baseline shifts, the true displacement wave was recovered by the velocity integrated displacement after de-trending a linear correction. The series of validation results have shown that, this method can fast and accurate retrieve the coseismic wave, the convergence time is smaller than one minute, and the precision are better than 2 mm/s and 2.5 cm for velocity and displacement respectively.

Keywords GPS and strong-motion combined measurements · Broadcast ephemeris · Coseismic wave retrieving · Real-time

19.1 Introduction

Strong-motion sensor is a kind of acceleration survey equipment, it with advantages of low-cost and high sensitivity, and is commonly used for earthquake monitoring and early warning [1–4]. However, it can only provide high-precision acceleration waves, the velocity and displacement waves are obtained by the acceleration integration [5–7]. As the tilting and/or rotation and some other reasons, the strong-motion records probably contain baseline shifts, they will be

R. Tu (✉)

The Germany Research Center for Geosciences, Telegrafenberg 14473 Potsdam, Germany
e-mail: turui-2004@126.com

further amplified if integrate into velocity or displacement. Currently, many empirical methods are used for the baseline shift correction [8–12]. But most of them involve large and unquantifiable uncertainties compare with the geodetic survey results, and can not be operated in real-time.

With the development of space geodesy technology, especially for the GPS, it has been an essential measurements for real-time earthquake monitoring and early warning. The Precise Point Positioning (PPP) and network solution are two basic solution models to retrieve high precision displacements. However, as the problems of the GPS system designs and receiver sampling rate, the GPS can only obtain high precision displacement, the velocity and acceleration are easily polluted by the high-frequency noises [5–7].

How to use the GPS, strong-motion combined measurements and complement the advantages of each other, make it neither affects by the strong-motion's baseline shifts nor affects by the GPS noise pollution and can provide high precision coseismic information is a hot topic in GPS seismology. Currently, many researchers have studied an integrated processing of high-rate GPS and strong-motion records, their researches can be classified into two categories. The first one is loose integration, it mainly use the high-precision GPS displacement to correct the baseline shift and recover the coseismic waves, such as [13, 14, 15]. The second one is tight integration, the coseismic waves are directly estimated by the GPS and acceleration raw observations, such as [16, 17, 15].

For these integration methods, one important condition is that the GPS observation must be with high precision. The network solution can provide the relatively displacement with mm precision, but it needs many reference stations for simultaneous observation and is difficult for real-time operation [13]. The dynamic PPP technology can provide the absolute displacement with cm precision, but needs a long time initialization [18, 19]. In additional, the data solution needs high-precision ephemeris and with poor timeliness.

For the application of earthquake monitoring and early warning, the goals are not only accurate and reliable, but also are easy for real-time operation and with high efficient. Based on these backgrounds, this paper propose an approach of real-time and fast retrieving the coseismic wave by GPS, strong-motion combined measurements and broadcast ephemeris. Firstly, the velocity observation equations and state equations of the strong-motion measurements are introduced into the PPP solution model, the baseline shifts of the strong-motion are real time estimated as unknown parameters like other positioning parameters by a Kalman filter. Then, the true velocity wave was retrieved by correcting the estimated baseline shifts, the true displacement information was retrieved by the velocity integrated displacement after de-trending a linear correction. The experimental and real earthquake data validation results have shown that, it can fast and accurate retrieve the coseismic waves.

19.2 Methodology

The approach is based on GPS, strong-motion combined measurements and broadcast ephemeris product, the dynamic PPP was used to estimate the baseline shift while adding the strong-motion observation firstly, then the coseismic wave was recovered by correcting the baseline shift and de-trending the linear correction. In this paper, the acceleration records of the strong-motion were firstly removed the initial baseline shift and integrated into velocity for the combined solution to recover the coseismic waves.

19.2.1 Mathematical Model

While the GPS using the ionosphere-free observation and consider the strong-motion's baseline shifts, the observation equations of the tight integration model can be written as following.

$$\begin{bmatrix} L_c \\ P_c \end{bmatrix}_k = \begin{bmatrix} e_k & m_{z,k} & 1 & 1 \\ e_k & m_{z,k} & 1 & 0 \end{bmatrix} \begin{bmatrix} x_k \\ z_k \\ \delta t_k \\ b \end{bmatrix} + \begin{bmatrix} \varepsilon_{Lc} \\ \varepsilon_{Pc} \end{bmatrix}, \quad \begin{matrix} \varepsilon_{Lc} \sim N(0, \delta_{Lc}^2) \\ \varepsilon_{Pc} \sim N(0, \delta_{Pc}^2) \end{matrix} \quad (19.1)$$

$$v_k = \dot{x}_k - u_k + w_{vk} \quad (19.2)$$

where, L_c and P_c are the observed minus computed phase and pseudorange observations from satellite to receiver respectively. v and u represent the strong-motion velocity observation and baseline shift. e is the unit direction vector from satellite to receiver. m is the wet tropospheric mapping function x , \dot{x} denotes the vector of the receiver position and velocity. $z, \delta t, b$ are the tropospheric zenith delay, receiver clock and phase ambiguities. ϵ is the measurement noise, its variances is δ^2 . k is the epoch number. The error components such as the antenna center offsets and variations, relativistic effect, tide loading and phase wind-up can be corrected with the existing methods [20, 21]. The baseline shifts are estimated as a random walk process, some other parameters like troposphere, receiver clock and phase ambiguities are treated the same as the traditional PPP.

The state equations for the station movement and baseline shifts are expressed as follows.

$$\begin{bmatrix} x_k \\ \dot{x}_k \\ u_k \end{bmatrix} = \begin{bmatrix} I & 0.5I\tau & 0.5I\tau \\ 0 & I & 0 \\ 0 & 0 & I \end{bmatrix} \begin{bmatrix} x_{k-1} \\ \dot{x}_{k-1} \\ u_{k-1} \end{bmatrix} + \begin{bmatrix} 0.5I \\ I \\ 0 \end{bmatrix} [v_k] + w_k \quad (19.3)$$

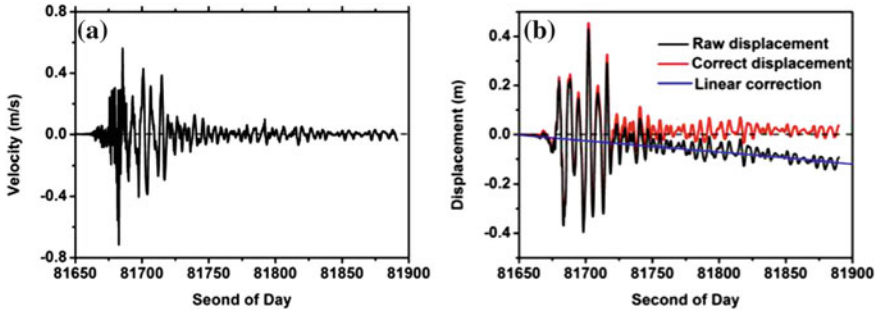


Fig. 19.1 De-trending the linear correction (**a** represents the recovered velocity, **b** represents de-trending the shift by a linear correction)

where, τ is the smallest sampling rate of the integrated sensors. w_k is the dynamic noise; with the expectation $E(w_k) = 0$ and variance

$$D(w_k) = \begin{bmatrix} \frac{\tau^3}{3} q_u^2 I & \frac{\tau^2}{2} q_u^2 I & 0 \\ \frac{\tau^2}{2} q_u^2 I & \tau q_u^2 I & 0 \\ 0 & 0 & \tau q_u^2 I \end{bmatrix}$$

respectively, q_u is the power density of the

baseline shift.

With these equations, a Kalman filter can be employed to solve the baseline shifts and some other parameters [22]. It is emphasized that as the GPS sample rate usually not matches the strong-motion’s sample rate, so the filter can only be employed on the GPS sample points, otherwise only for the prediction [23].

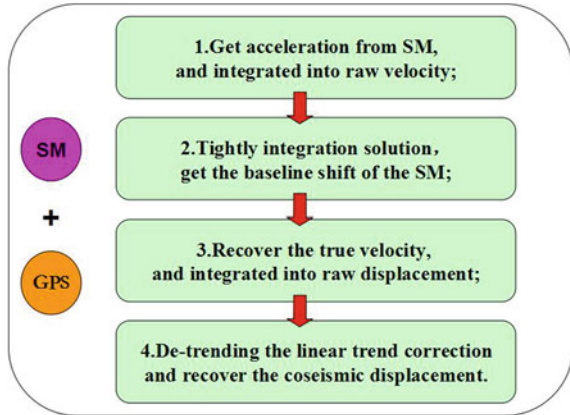
19.2.2 De-Trending the Linear Correction

As the broadcast ephemeris with a low precision and the ambiguities and atmosphere parameters can not estimate accurately in a short period, the solved baseline shift may have a constant bias. It will results in the corrected velocity with a bias, it is smaller than 2 mm/s and can be negligible for the inversion analysis (shown in Fig. 19.1a). But it will lead to a large linear trend while integrated into displacement, as shown in Fig. 19.1b (in black). The trend is very stable in a short period and can be removed easily by a linear correction (in blue), then the coseismic displacements are recovered (in red).

19.2.3 The Implementation Process of the Combined System

Figure 19.2 shows the implementation flow of the approach. The first step, retrieve the high-frequency acceleration records from the strong-motion measurements, and integrated into velocity after remove the initial baseline shifts. The second

Fig. 19.2 The flow of the combined system



step, estimate the strong-motion's baseline shift by the tight integration of GPS raw observation and strong-motion velocity. The third step, recover the true velocity by correcting the estimated baseline shift and integrated it into raw displacement. The fourth step, de-trend the linear trend correction and recover the coseismic displacement.

19.3 Validation and Analysis

The following data was used for validation and analysis. The data is processed in a simulated real-time mode, and the broadcast ephemeris was used for data solution. The acceleration records of the strong-motion were removed the initial shifts by the empirical method of [12] firstly, then integrated into velocity time series for the combined solution.

19.3.1 Analysis of the Experimental Data

Firstly, the experimental dataset which carried out on December 2012 at GFZ was used for the validation. It contains a platform, which can be slide along a table, includes a dynamic GPS antenna, and a strong-motion sensor, the details can be found in [15]. The sampling rates are 50 and 100 Hz for the GPS and the strong-motion sensor respectively, we simulated eight simulations, the GPS data was utilized to 1 Hz for the data analysis. In Fig. 19.3, the left side shows the raw integrated velocity (black) and the estimated baseline shift (red). We can clearly see that for the eight simulations, they all have large baseline shift and the integrated velocity are seriously polluted. The middle side shows the time series of the corrected velocity, the velocity was shaken between the zero line when there is no

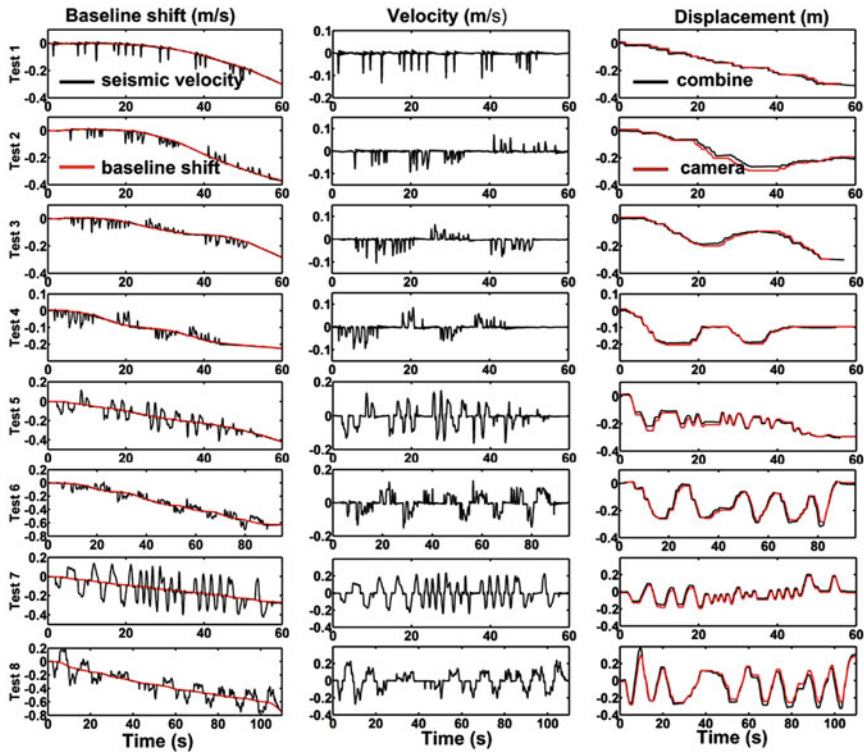


Fig. 19.3 The combined results of the eight simulations

movement, comparison to the raw velocity, it is corrected very well. The right side shows the recovered displacement (in black) and the reference displacement (in red) which provided by the high-frequency camera with a precision of 3 mm, they are consistent with each other very well.

19.3.2 Analysis of the Real Earthquake Data

Furthermore, we collected the co-located GPS and seismic data during the E1 Mayor-Cucapah earthquake (Mw 7.2, 4 April 2010, 22:40:42 UTC) to estimate the three-dimensional (3D) baseline shifts and recover the coseismic velocity and displacement. Four pairs of co-located GPS and strong-motion seismometer are selected and processed. The GPS station P496, which is located 73 km from the earthquake epicenter, is co-located with the seismic station 0931 of the Southern California Seismic Network (SCSN) with a distance of about 10 km. GPS station P496 located 74 km from the epicenter is about 140 m away from its co-located

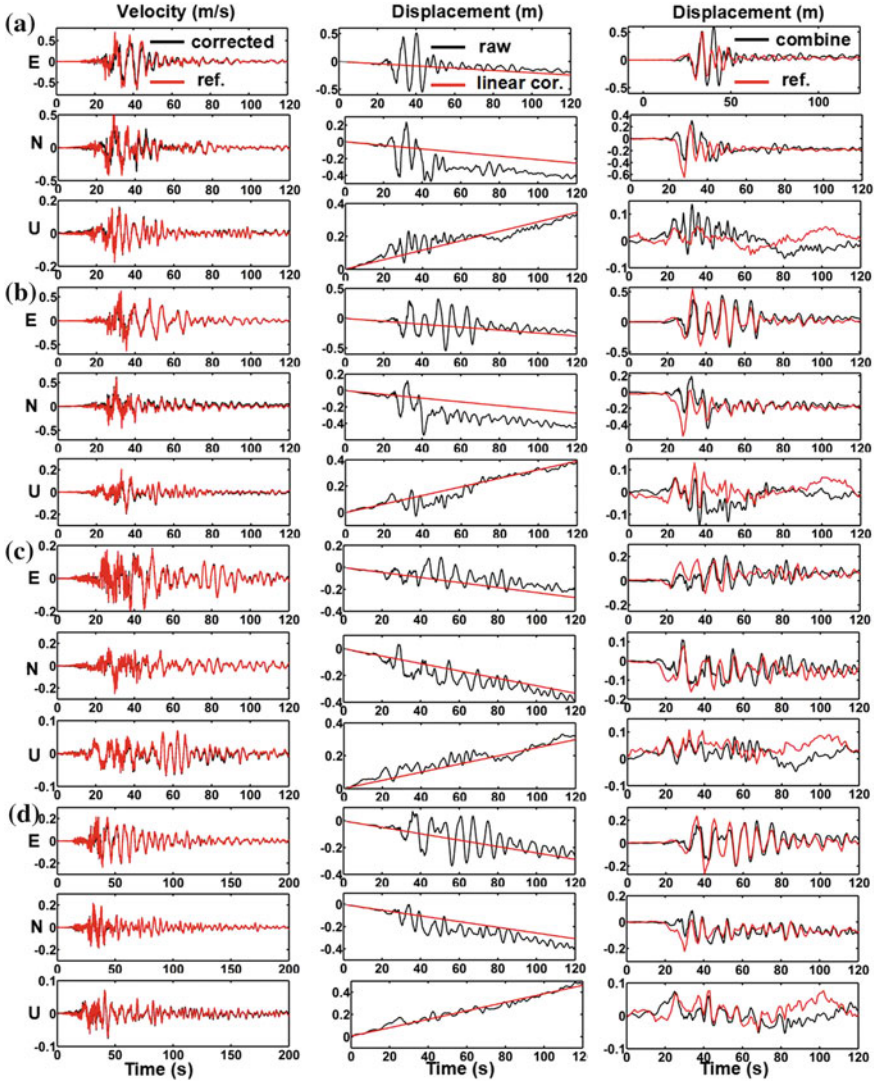


Fig. 19.4 The results of the four combined pairs (a, b, c, d represents the combined pairs of P494/0931, P496/5058, P500/5054, P744/5028 respectively)

seismic station 5058. GPS station P500 located 63 km from the epicenter is about 3.6 km away from its co-located seismic station 5054. GPS station P744 located 80 km from the epicenter is about 275 m away from its co-located seismic station 5028. The accelerometer data is 200 Hz, and the GPS data is recorded at 5 Hz. Figure 19.4a–d are the results of the four pairs (P494/0931, P496/5058, P500/5054, P744/5028) in ENU components. The left side are the velocity comparison, where the reference velocity (red) was provided by the USGS post solution

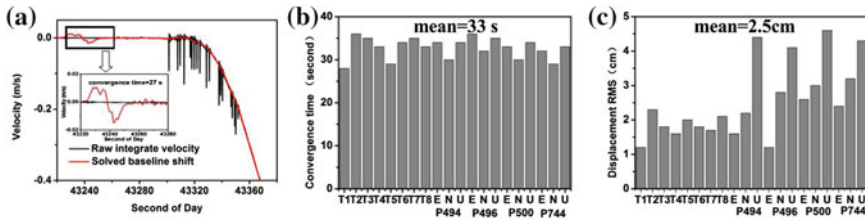


Fig. 19.5 a presents the convergence process of the estimated baseline shift, b,c presents the statics of the convergence time and precision respectively

(http://nsmg.wr.usgs.gov/datasets/20100404_2240.html), we can concluded that the recovered velocity waves are consistent with the USGS references. The middle side shows the raw integrated displacement (in black) and the linear correction (in red). The right side shows the comparison of the de-trend displacement (in black) and the GPS post solution displacement (in red). The real-time and fast retrieved displacement are well consistent with the post solutions in horizontal component, while in vertical component, as the atmosphere error is difficult to process, the recovered displacement with large uncertainties.

19.3.3 The Analysis of the Convergence and Precision

Figure 19.5 shows the convergence time and the RMS values of the displacement bias, where the convergence time was statical by the bias of the solved baseline shift is smaller than 2 mm/s (in Fig. 19.5a, the red color represents the solved baseline shift, the black color represents the integrated velocity). The camera recorded movement tracks (the precision is better than 3 mm) were used for the simulated experimental precision analysis, and for the real earthquake, the GPS post solution (the precision is better than 1 cm) was used as a reference. From the Fig. 19.5b, c the average convergence time is 33 s for the combined system, and the precision of recovered displacement is 2.5 cm, it is much better than the traditional PPP solutions.

19.4 Conclusions

This paper propose an approach of real-time and fast retrieving the coseismic wave by GPS, strong-motion combined measurements and broadcast ephemeris. In this method, the acceleration of the strong-motion was integrated into velocity firstly, then tightly integrated with the GPS raw observations to estimated the strong-motion’s baseline shifts, finally the true coseismic wave was recovered by correcting the baseline shifts and removing a linear correction. After introducing the

algorithms, we make a validation analysis by two different datasets. The series results have shown that, the baseline shifts of the strong-motion are recognized and corrected effectively, and high-precision coseismic information is recovered, the precision are better than 2 mm/s and 2.5 cm for velocity and displacement respectively. Compare with some other combination methods, this approach not only has a short convergence time but also can provided high-precision and broadband displacement, velocity and acceleration waves. Compare with empirical baseline shift correction methods, which using the empirical double broken line to correct the velocity, the present method real-time estimated and corrected the transient baseline shifts, it is more objective and accurate. In additional, the data solution using the broadcast ephemeris and stand-alone data, it is easy for real-time application.

References

1. McComb HE, Ruge AC, Neumann F (1943) The determination of true ground motion by integration of strong-motion records: a symposium. *Bull Seismol Soc Am* 33:1–63
2. Graizer VM (1979) Determination of the true ground displacement by using strong motion records. *Izv Earth Phys* 25:26–29
3. Chiu H (1997) Stable baseline correction of digital strong-motion data. *Bull Seism Soc Am* 87:932–944
4. Zhu L (2003) Recovering permanent displacements from seismic records of the June 9, 1994 Bolivia deep earthquake. *Geophys Res Lett* 30:1740. doi:[10.1029/2003GL017302](https://doi.org/10.1029/2003GL017302)
5. Elósegui P, Davis JL, Oberlander D, Baena R, Ekström G (2006) Accuracy of high-rate GPS for seismology. *Geophys Res Lett* 33:L11308. doi:[10.1029/2006GL026065](https://doi.org/10.1029/2006GL026065)
6. Genrich JF, Bock Y (2006) Instantaneous geodetic positioning with 10–50 Hz GPS measurements: noise characteristics and implications for monitoring networks. *J Geophys Res* 111:B03403. doi:[10.1029/2005JB003617](https://doi.org/10.1029/2005JB003617)
7. Larson KM, Bilich A, Axelrad P (2007) Improving the precision of high-rate GPS. *J Geophys Res* 112:B05422. doi:[10.1029/2006JB004367](https://doi.org/10.1029/2006JB004367)
8. Iwan W, Moser M, Peng C (1985) Some observations on strong-motion earthquake measurement using a digital accelerometer. *Bull Seism Soc Am* 75:1225–1246
9. Boore DM (2001) Effect of baseline corrections on displacement and response spectra for several recordings of the 1999 Chi-Chi, Taiwan, earthquake. *Bull Seism Soc Am* 91:1199–1211
10. Graizer V (2006) Tilts in strong ground motion. *Bull Seism Soc Am* 96:2090–2106
11. Wu Y, Wu C (2007) Approximate recovery of coseismic deformation from Taiwan strong-motion records. *J Seismol* 11:159–170
12. Wang R, Schurr B, Milkereit C, Shao Zh, Jin M (2011) An improved automatic scheme for empirical baseline correction of digital strong-motion records. *Bull Seism Soc Am* 101:2029–2044
13. Bock Y, Melgar D, Crowell BW (2011) Real-time strong-motion broadband displacements from collocated GPS and accelerometers. *Bull Seism Soc Am* 101:2904–2925
14. Wang R, Parolai S, Ge M, Jin MP, Walter TR, Zschau J (2013) The 2011 Mw 9.0 Tohoku earthquake: comparison of GPS and strong-motion data. *Bull Seism Soc Am*. doi:[10.1785/0120110264](https://doi.org/10.1785/0120110264)
15. Tu R, Wang R, Ge M, Walter TR, Ramatschi M, Milkereit C, Bindi D, Dahm T (2013a) Cost effective monitoring of broadband strong ground motion related to earthquakes, landslides or

- volcanic activities by joint use of a single-frequency GPS and a MEMS-type accelerometer. *Geophys Res Lett.* doi:[10.1002/grl.50653](https://doi.org/10.1002/grl.50653)
16. Geng J, Bock Y, Melgar D, Crowell BW, Haase JS (2013) A new seismogeodetic approach applied to GPS and accelerometer observations of the 2011 Brawley seismic swarm: implications for earthquake early warning. *Geophys Geosyst, Geochem.* doi:[10.1002/ggge.20144](https://doi.org/10.1002/ggge.20144)
 17. Li X, Ge M, Zhang Y, Wang R, Klotz J, Wicket J (2013) Tightly integrated processing of high-rate GPS and strong-motion data: Application to earthquake early warning. *Geophys J Int.* doi:[10.1093/gji/ggt249](https://doi.org/10.1093/gji/ggt249)
 18. Zumberge JF, Heflin MB, Jefferson DC, Watkins M (1997) Precise point positioning for the efficient and robust analysis of GPS data from large networks. *J Geophys Res* 102:5005–5017
 19. Bisnath S., Gao Y (2007) Current state of precise point positioning and future prospects and limitations. *Observing our changing earth, international association of Geodesy Symposia* 133, Springer-Verlag, Berlin Heidelberg
 20. Dach R, Hugentobler U, Fridez P, Michael M (eds) (2007) *Bernese GPS software version 5.0.* Astronomical Institute, University of Bern
 21. Kouba J, Héroux P (2001) Precise point positioning using IGS orbit and clock products. *GPS Solut* 5(2):12–28. doi:[10.1007/PL00012883](https://doi.org/10.1007/PL00012883)
 22. Tu R, Ge M, Wang R, Walter TR (2013) Real-time seismic data processing: a new algorithm for tight integration of high-rate GPS and strong-motion records, demonstrated for experimental data and the 2010 Baja California earthquake (Mw 7.2). *J Seismol.* doi:[10.1007/s10950-013-9408-x](https://doi.org/10.1007/s10950-013-9408-x)
 23. Smyth A, Wu M (2006) Multi-rate Kalman filtering for the data fusion of displacement and acceleration response measurements in dynamic system monitoring. *Mech Syst Signal Process* 21:706–723